Effect of 10% recycled sands from various storage sites on the mortar's properties

Left running head: E. GHORBEL ET AL.

Short title : European Journal of Environmental and Civil Engineering

AQ0

Elhem Ghorbel[a], George Wardeh[a] and AQ7 [ID] Belén González-Fonteboa[b]

[a]L2MGC, CY Cergy-Paris University, Neuville-sur-Oise, France;

[b]Department of Civil Engineering, Universidade da Coruña, E.T.S.I. Caminos, A Coruña, Spain

Corresponding Author

CONTACT Elhem Ghorbel Elhem.ghorbel@cyu.fr L2MGC, CY Cergy-Paris University, Neuville-sur-Oise, 95031, France. **AQ1**

Abstract

This study investigates the effects of using 10% of recycled sand in mortars. Using the concrete equivalent mortar approach, the reference mortar was developed from a flowable natural aggregate concrete with a C35/45 strength class. Five mortars were manufactured by replacing 10% of the natural sand with recycled sand from various recycling platforms while keeping the formulation parameters constant. The fresh state results showed that recycled mortar had an increased air content, which increased yield stress and viscosity. In addition, mortars containing 10% recycled sand showed a faster rate of flow loss over time. There was no difference between the materials in the hardening state with regard to the evolution of the hydration heat or the setting time. The relationship between the qualities of mortars and sands revealed that the air content depends on the sand's fineness and the presence of fines with a diameter less than 63 μm. A relatively small increase in porosity and water absorption capacity was observed with a decrease in the compressive and flexural strength with no obvious change in the elastic modulus. The total shrinkage was revealed to depend on the fines content and decreases when the fines content increases.

KEYWORDS

Mortar; recycled sand; workability; physical properties; mechanical properties ✍

1. Introduction

The French construction industry produces more than 40 million tonnes of waste annually, of which 80% are inert, 23% are non-hazardous and 2% are dangerous (Ecological Transition Agency, 2020; UNPG, 2015). In parallel, this industry uses 80 million tons of aggregates, or 17% of French total production, to meet the demands of renovation and new building (UNPG, 2015). Demolition, new building and rehabilitation were the three categories used to classify the sites in this sector. The sites that generate the most waste (65%) are those involved in demolition, followed by those engaged in restoration (28%), and those invest in new construction (7%) (Ecological Transition Agency, 2020; Haeusler & Berthoin, 2015). In the context of sustainable development and tightening landfill regulations, concrete waste is now converted into so-called recycled aggregates rather than natural ones. These aggregates are obtained through crushing and grinding, either on a fixed installation or right on the job site using a mobile crusher. The objectives set forth by the Waste Directive 2008/98/EC and the Energy Transition Law for Green Growth of August 2015, in particular, place recycling of these wastes at the centre of national and European legislation. Reusing waste is completely in line with the principles of the circular economy connected to sustainable development and environmental protection. The use of circular economy principles for effective waste management enables the preservation of primary natural resources as well as the maintenance of secondary resources in the production cycle (Bao et al., 2019; Fořt & Černý, 2020; Ginga et al., 2020; Sanguino et al., 2020; Yu et al., 2021).

After being crushed, the cement paste that surrounds the natural grains in recycled aggregates stays adherent (de Juan & Gutiérrez, 2009; Ghorbel et al., 2020). This adherent layer has a higher water absorption capacity since it is more porous and less dense than natural grains (de Juan & Gutiérrez, 2009; Ghorbel et al., 2019; Wardeh et al., 2015). Indeed, a number of production factors, such as the crushing process and the calibre of the original concrete, affect the characteristics of recycled aggregates (Francois & Colina, 2019). Due to the concentration of old cement paste particles in the finest granular fraction caused by concrete crushing, recycled sand composition exhibits high heterogeneities (Francois & Colina, 2019). As a result, compared to coarse recycled aggregates, recycled sands have higher water absorption and lower actual density (Omary et al., 2016; Omary et al., 2018). The quality of the recycled aggregates also depends on the original material's quality, the crushing process and the efficiency of the production platform (Evangelista et al., 2015; Francois & Colina, 2019).

Although recycled sand's effects on the qualities of the finished material have not yet been fully understood, recycled coarse aggregates have the potential to completely replace natural aggregates in concrete (Ghorbel et al., 2019; Ghorbel et al., 2019; González-Fonteboa et al., 2012). Evangelista et al. examined the mineralogical and physical characteristics of fine recycled aggregates (Evangelista et al., 2015). The connected hydrates in recycled sand are different for each granular fraction, and as a result, each fraction absorbs water differently, as shown by Zhao et al. (2015). These specific sand properties directly affect These particular characteristics of sand have a direct influence on the workability and the fresh behaviour of mortars (Ghorbel

et al., 2019; Le et al., 2016). An experimental research on the impact of mix design parameters on the performances of mortars including various percentages of recycled sand was carried out by Ghorbel et al. (2019). Two sets of mortars were created in this work by replacing natural sand with a particular type of recycled sand at substitution percentages ranging from 0% to 100%. While the other series had constant workability and varied water to cement ratios (W/C), the first series had variable workability and constant W/C. The authors found that adding recycled sand considerably decreased the workability of mortars over time. This decrease was explained by the recycled sand's continuous absorption of the mixing water as well as by its higher aspect ratio and irregular shape when compared to natural sand. Zhao et al. (2013), Cuenca-Moyano et al. (2014) and Le et al. (2016) came to the same result and discovered that the initial workability of recycled sand mortars relies on the initial water content, pre-saturation method and pre-saturation time. Ghorbel et al. (2019) found that the density decreases while the air content increases with the substitution ratio for both series at the fresh state as well.

Numerous research in the literature have examined the effect of recycled sand on the mechanical performance of the mortar (Braga et al., 2012; Corinaldesi & Moriconi, 2010; Dapena et al., 2011; Ghorbel et al., 2019; Kim, 2021; Ledesma et al., 2015; Vegas et al., 2009; Zhang et al., 2018). When recycled sand content was increased to 20% in three series of mortars, Dapena et al. (2011) observed a drop in compressive strength of 25% in series 3 and a reduction in 21% in series 1 and 31% in series 2 at 28 days. Contrarily, Vegas et al. (2009), showed that the main characteristics of masonry mortars could be preserved with a 25% substitution of fine recycled concrete aggregates for natural sand. Depending on the source of the sand, the reduction in compressive and flexural strengths can reach 50% when natural sand is completely replaced with recycled one (Kim, 2021). Ghorbel et al. (2019) studied the mechanical properties of the two series of mortars developed in their work. They concluded that whereas mechanical properties decreased linearly for the series with initial constant workability, they decreased to a step starting from a replacement ratio of 30% for mortars with variable workability.

Within the framework of past investigations, the authors examined one type of recycled sand in practice (Braga et al., 2012; Corinaldesi & Moriconi, 2010; Cuenca-Moyano et al., 2014; Ghorbel et al., 2019; Kim, 2021; Ledesma et al., 2015; Vegas et al., 2009; Zhao et al., 2015). While Ghorbel et al. (2019) used one type of recycled sand in two series of mortars to study the effect of replacement ratios on the fresh and hardened properties, Cuenca-Moyano et al. (2014) used recycled fine aggregates produced in a C&DW treatment and recovery plant to assess the impact of pre-soaking on mortar performance. Braga et al. (2012), Zhao et al. (2015), Corinaldesi and Moriconi (2009) and Kim (2021) used one type of recycled fine aggregates to carry out their studies.

Based on the results of this survey, this study aims to determine whether 10% recycled sand incorporation has any impact on the physical and mechanical properties in both the fresh and hardened phases when 5 types of recycled sand from various recycling platforms were employed. The article attempts to address concerns about the actions that should or should not be performed if the substitution ratio is low, regardless of the recycling facility and without knowledge of the origins of the recycled sand.

2. Materials and methods

2.1. Materials

Raw materials used in this study were the following:

- A Portland cement type CEM II/A-L 42.5N with a specific gravity of 3.09 and a Blaine surface is of 3700m^2/kg. The compressive strength at 28 days, measured according to the standard NF EN 196-1 (NF EN 196-1, 2006), is higher than 53 MPa. The chemical and mineralogical compositions of the clinker are given in Table 1.

- Limestone fillers, known as Betocarb HP-OG, manufactured by OMYA SAS. Its bulk density, measured according to standard NF EN 1097-7 (NF EN 1097-7, 2008), is 2.7 kg/cm^3 and the Blaine surface is equal to 500 m^2/kg.

- MC PowerFlow 3140 superplasticizer.

- 0/4 mm natural sand (named NS 0/4) from the Lafarge quarry in Sandrancourt in the north west of Paris-France

- 5 types of recycled sand from different recycling platforms were used in this study named hereafter RS-0 to RS-IV. The origin of the recycled sand is as follows:
  - RS-0 from Gonesse platform located north of Paris.
  - RS-I from Neuilly platform at north of Paris.
  - RS-II from Leonhart platform located in eastern France near the borders with Germany. The sand RS-II was sieved in laboratory from 0/22.5 mm granular mixture.
  - RS-III from Anse platform in the south east of France in the Lyon region. The sand was sieved in laboratory from 0/20 mm mixture.
  - RS-IV from Ancycla platform in the south east of France in the Lyon region. The sand was also sieved in laboratory from 0/22.4 mixture.

Note: The table layout displayed in 'Edit' view is not how it will appear in the printed/pdf version. This html display is to enable content corrections to the table. To preview the printed/pdf presentation of the table, please view the 'PDF' tab.

Table 1. Chemical and mineralogical composition of the cement. ⊕

SiO$_2$	Al$_2$O$_3$	Fe$_2$O$_3$	CaO$_t$	MgO	SO$_3$	K$_2$O	CaO$_{free}$	(NA$_2$O)eq	PAF
18.7%	4.9%	3.7%	62%	1.3%	2.7%	0.68%	1.5%	0.59%	5.1%

Phase	C_3S	C_3A	C_4AF	C_2S
Mass fraction x_i	0.583	0.067	0.113	0.097

Place the cursor position on table column and click 'Add New' to add table footnote.

It is worth mentioning that all sands have been washed before sending to research organisations. The used sands are illustrated in Figure 1.

Figure 1. The different recycled sands used for the formulation of mortars. ⊕
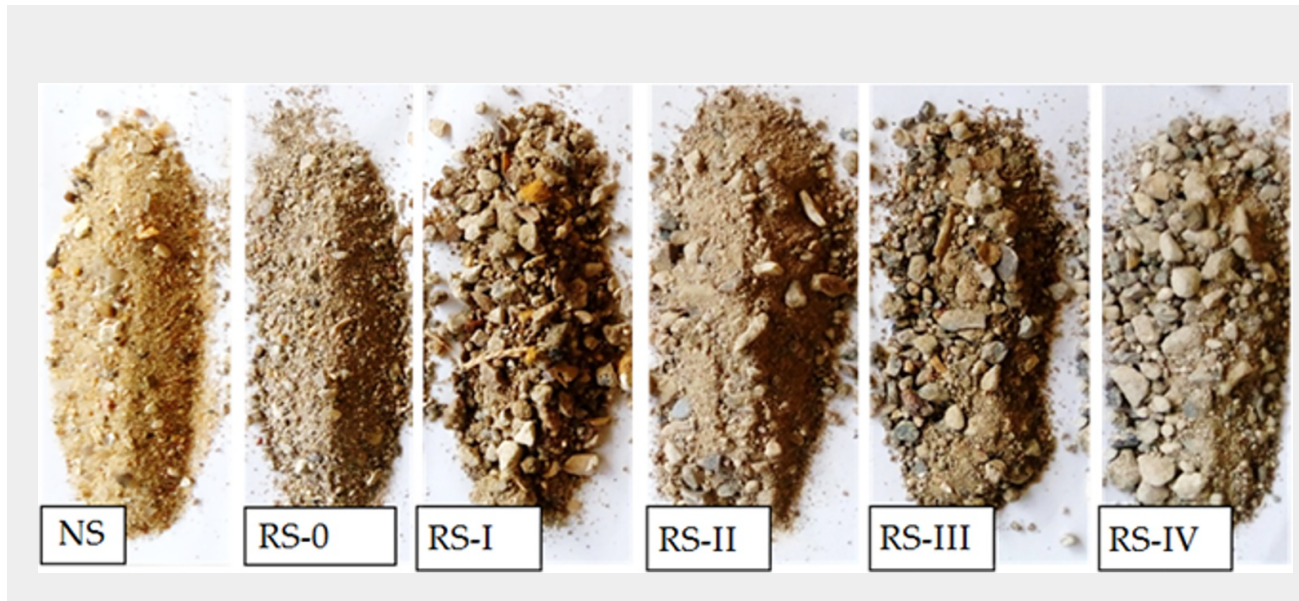
2.2. Physical properties of aggregates

The standard NF EN 933-1 (NF EN 933-1, 2012) was used to determine the particle size distribution of the sands depicted in Figure 2. The graph demonstrates that recycled sands have a tight particle size distribution, which differs from the natural sand distribution.

Figure 2. Particle size distribution of used sand. ⊕
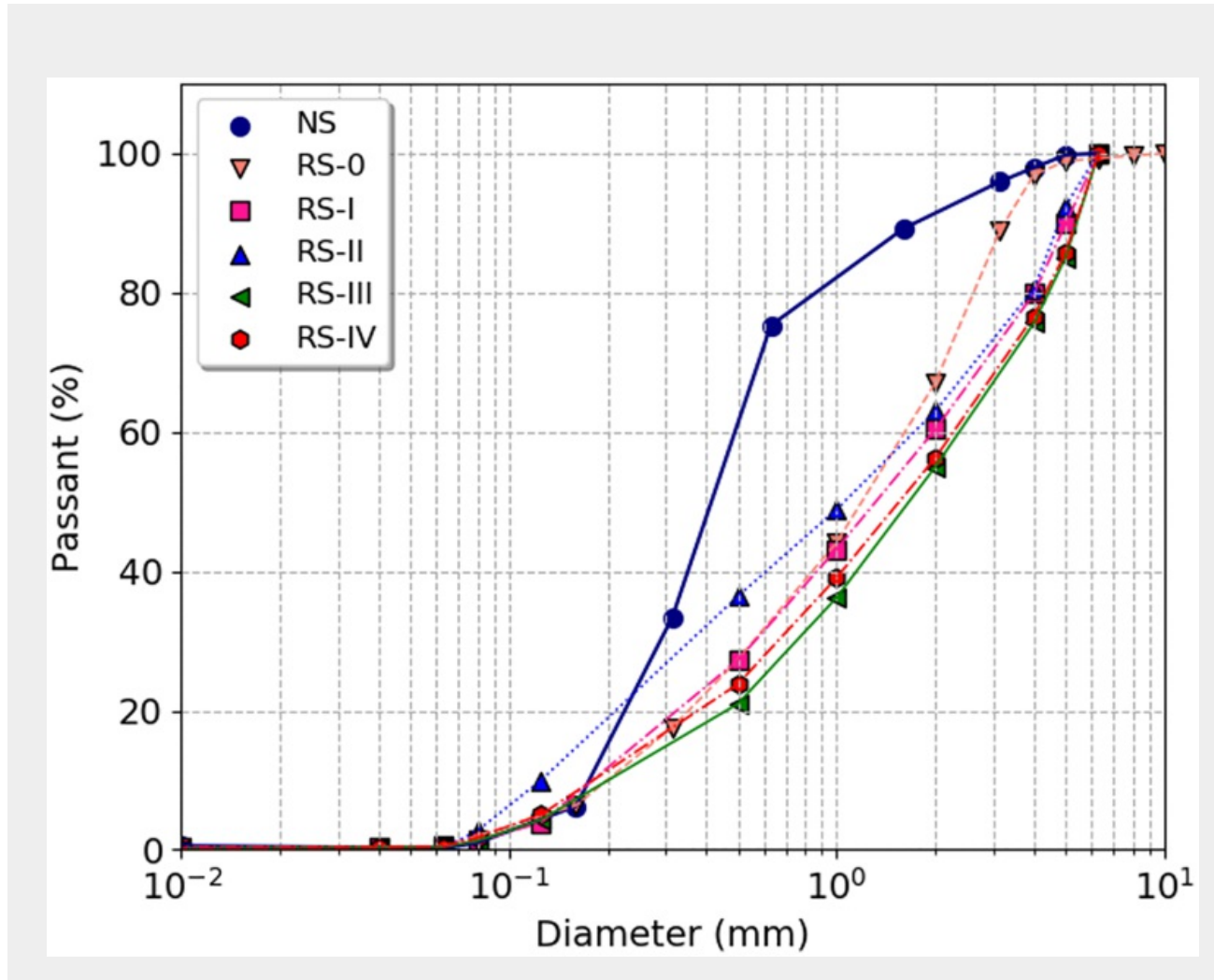
To calculate the bulk oven-dry specific gravity and water absorption of sands, the standard NF EN 1097-6 (NF EN 1097-6, 2014) was used. The fineness modulus was calculated based on the percentages of material retained on a predetermined sequence of sieves and using the standard NF EN 13139 (NF EN 13139, 2003). The relative quantities of clay-size or plastic fines and dust in sand were calculated using the sand equivalent test, which was carried out in accordance with the standard NF EN 933-8 (NF EN 933-8 + A1, 2015).

The aforementioned characteristics are summarised in Table 2, where it is obvious that all recycled sands include less than 3% by mass of fines lower than 63 μm. The finesse modulus of sand RS-III and RS-IV is

the lowest, and all recycled sands have higher porosities and absorption coefficients than natural sand. The highest porosities and absorption coefficients are found in sands RS-I, RS-II and RS-IV. Figure 3 shows the relationship between the water absorption coefficient and the proportion of fines less than 63 μm for the sands used in the current study, together with previous results from the literature (Cuenca-Moyano et al., 2014; Ghorbel et al., 2019; Berredjem et al., 2018; Saiz-Martínez et al., 2015; Velay-Lizancos et al., 2018; Zega et al., 2010). According to Zhao et al., the presence of the old cement paste adhered to the sand particles causes the water absorption to be proportional to the fine content (Zhao et al., 2013). The difference between the experimental points and those of the literature can be explained by the washing of the sand in the present work.

Figure 3. Water absorption versus the percentage of fines lower than 63 μm. ⊕
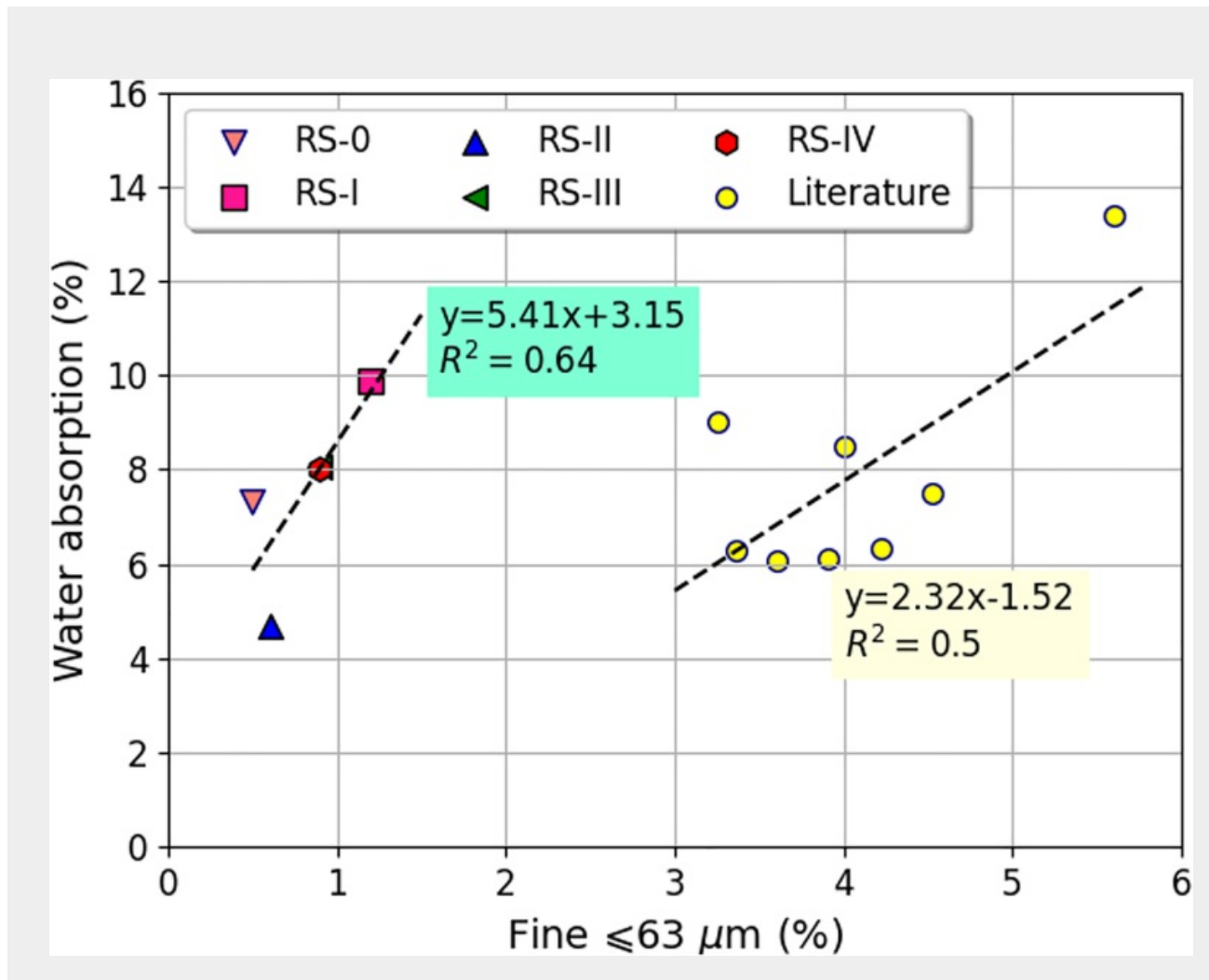
Figure with axes: x-axis "Fine ⩽63 μm (%)" ranging 0 to 6; y-axis "Water absorption (%)" ranging 0 to 16. Legend: RS-0, RS-I, RS-II, RS-III, RS-IV, Literature. Equations on plot: $y=5.41x+3.15$, $R^2 = 0.64$ and $y=2.32x-1.52$, $R^2 = 0.5$.

Note: The table layout displayed in 'Edit' view is not how it will appear in the printed/pdf version. This html display is to enable content corrections to the table. To preview the printed/pdf presentation of the table, please view the 'PDF' tab.

Table 2. Physical properties of sand. ⊕

Property	Natural sand	Recycled sand				
	NS	RS-0	RS-I	RS-II	RS-III	RS-IV
Plaetform	Sandrancourt	Gonesse	Neuilly	Leonhart	Anse	Ancycla
Bulk density ρssd (kg/m3) NF EN 1097-6 [4]	2654 ± 39	2366 ± 42	2373 ± 10	2683 ± 43	2565 ± 24	2386 ± 21

Water absorption WA24 (%) NF EN 1097-6 [33]	0.89 ± 0.10	7.32 ± 0.11	9.86 ± 0.27	4.67 ± 0.73	8.08 ± 0.11	8.03 ± 0.86
Fineness modulus NF EN 13139 [34]	2.42 ± 0.04	3.46 ± 0.05	3.73 ± 0.02	3.41 ± 0.16	3.98 ± 0.01	3.87 ± 0.04
Percentage of fines ≤63 μm	0.4 ± 0.01	0.5 ± 0.01	1.2 ± 0.01	0.6 ± 0.2	0.9 ± 0.05	0.9 ± 0.4

Place the cursor position on table column and click 'Add New' to add table footnote.

2.3. Mortar mix design

To examine the impact of fine recycled aggregate incorporation on mortar characteristics at fresh and hardened states, the concrete equivalent mortar (CEM) method (Ghorbel et al., 2019; Schwartzentruber & Catherine, 2000) was used. Six CEMs were evaluated, including one reference mortar made with natural sand and five with 10% by volume replacement ratio of natural sand by recycled sands. Reference mortar corresponds to the concrete equivalent mortar of a natural aggregate concrete with a slump flow equal to 180 ± 20 mm (S4 consistency class according to the standard NF EN 206/CN (NF EN 206-1, 2014)) and C35/45 compressive strength class according to the standard NF EN 206/CN (NF EN 206-1, 2014)). The composition of the reference concrete was studied in detail in the authors' previous work (Safiullah Omary et al., 2018; Wardeh & Ghorbel, 2019; Wardeh et al., 2017) and is summarised in Table 3. According to the nomenclature C35/45-0S-0G, there is no replacement of sand and no replacement of gravel.

Note: The table layout displayed in 'Edit' view is not how it will appear in the printed/pdf version. This html display is to enable content corrections to the table. To preview the printed/pdf presentation of the table, please view the 'PDF' tab.

Table 3. Mix proportions of reference concrete mixture. ⊕

Components (kg/m3)	C35/45-0S-0G
Total water	185
Effective water	175
Cement	299

Fillers	58
Natural sand	771
Recycled sand	–
Natural gravel (4/10)	264
Recycled gravel (4/10)	–
Natural gravel (6.3/20)	810
Recycled gravel (10/20)	–
Superplasticizer	1.89
Effective water/Binder (W/B)	0.49
Paste volume (m3)	0.29

Place the cursor position on table column and click 'Add New' to add table footnote.

Because the volume of water and the surface of solid components are conserved, there is a linear correlation between the workability of the CEM and that of concrete from a rheological point of view. In fact, the flow as measured by the mortar scale is equivalent to the slump of the concrete (Ghorbel et al., 2019; Mohamed et al., 2010). The CEM formulation approach is reduced to the determination of a developed surface by aggregates which are modelled as perfectly spherical particles in order to simplify the calculation of the surface and the volume of each granular class. For the class whose diameter is d_i, the volume is given by $v_i = \frac{\pi d_i^3}{6}$ and the surface is given by $s_i = \pi d_i^2$. The mass of aggregates in each granular slice is given by $M_i = (R_{mi} - R_{Mi})\frac{g}{100}$ where g (kg/m^3) is the content of aggregate in the concrete mixture while R_{mi} and R_{Mi} are the rejects associated to the upper and lower sieve defining a granular slice i. The volume of aggregates contained in the slice, i, is given by $V_i = \frac{M_i}{\rho}$ and the number of particles is expressed by $N_i = \frac{V_i}{v_i}$ where ρ is the density. Finally, the developed surface for the slice, i, is given by $S_i = N_i s_i = \frac{V_i}{v_i} \times s_i$ and the total developed surface is the sum of developed surfaces for all granular slices. CEM calculation consists in replacing the coarse aggregates with sand whose developed surface is equal to that of coarse aggregates. Table 4 recapitulates the mix proportions of all derived CEM which are described as follow:

Note: The table layout displayed in 'Edit' view is not how it will appear in the printed/pdf version. This html display is to enable content corrections to the table. To preview the printed/pdf presentation of the table, please view the 'PDF' tab.

Constituent (kg/m^3)	M-SN	M-RS-0	M-RS-I	M-RS-II	M-RS-III	M-RS-IV
Cement	481.7	481.7	481.7	481.7	481.7	481.7
Filler	93.4	93.4	93.4	93.4	93.4	93.4
Water	298.1	298.1	298.1	298.1	298.1	298.1
Natural sand	1299.1	1169.9	1169.9	1169.9	1169.9	1169.9
Recycled sand	0.0	112.3	109.0	131.8	111.8	113.0
Superplasticizer	3.2	3.2	3.2	3.2	3.2	3.2

Table 4. Mix proportions of mortars. ⊕

Place the cursor position on table column and click 'Add New' to add table footnote.

- M-SN: material with natural sand
- M-RSx: mortar with 10% of recycled sand number x

2.4. Test methods

2.4.1. Properties of fresh mortars

The test procedure outlined in NF EN 1015-6 (NF EN 1015-6, 1999) was used to determine the density of fresh mortars. The air content was determined using the test procedure specified in NF EN 1015-7 (NF EN 1015-7, 1999) and 1 litre air content metre CONTROLS in accordance with BS EN 459-2 (BS EN 459-2, 2010).

The slump test performed according to NF EN 12350-2 (NF EN 12350-2, 2010) was used to control the workability of mortars and the evolution of their normalised slump over time. The slump is measured using a special mini-cone adopted for CEM characterisation whose dimensions are deduced from Abram's cone by a homothetic ratio of two (Upper diameter ϕ_{upper} = 50 mm, lower diameter ϕ_{lower} =100 mm and height h = 150 mm) (Ghorbel et al., 2019; Mohamed et al., 2010; Schwartzentruber & Catherine, 2000).

According to the standard NF EN 480-2 (NF EN 480-2, 2006), the setting time of mortars was measured using the traditional Vicat apparatus that had an additional 700 g of mass added to it. The flow time of mortars was also measured using the Marsh whose dimensions are: height of 315 mm, upper diameter of 160 m and lower diameter of 12 mm with a 45 mm high nozzle. The test consists of measuring the time that a certain volume of the fluid material takes to flow through the nozzle (NF P18-507, 1992; Roussel & Coussot, 2005).

From the mortar cone results the yield stress can be calculated according to the following expression proposed by Bouvet et al. (2010):

| $$\tau_0 = \frac{225\rho g V^2}{4\pi^2 d^5}$$ | Equation 1 |

with ρ the fresh density of mortar, g the gravity and V the volume of the tested material and d the flow given by the diameter of the formed wafer.

According to the same authors, the viscosity μ_0 can be calculated based on the yield stress and the flow time called t_f (Eq. 2).

| $$\mu_0 = \tau_0 \left(6.41 \times t_f - 1.94\right) \times 10^{-3}$$ | Equation 2 |

According to the standard NF EN 196-9 [52], the hydration heat measurement was performed using a semi-adiabatic calorimeter in a climate-controlled chamber at a controlled temperature of 20 °C. The thermocouples of the calorimeter were connected to a multi-channel measurement chain with microprocessors allowing temperatures to be stored during tests. The heat of hydration, named Q (J/g), at the instant t, is given by the following form:

| $$Q = \frac{c}{m_c}\theta + \frac{1}{m_c}\int_0^t \alpha\theta_i \, dt$$ | Equation 3 |

where α is the heat loss coefficient and θ is the temperature.

2.4.2. Properties of hardened mortars

The porosity, flexural strength, compressive strength and dynamic modulus of elasticity of hardened mortars are the properties that have been examined. The test for water-accessible porosity was conducted in accordance with the method recommended by standard NF P18-459 (NF P18-459, 2010). It was determined for each mortar on three cubic samples (40x40x40 mm^3) after preservation in water at room temperature for 28 days. The samples were placed under vacuum for 4 hours at a pressure equal to 25 mbar and then they were immersed in water at this pressure for 44 hours. After 48 hours, the resulting mass was measured by hydrostatic weighing and then the dry mass was determined after drying at a temperature of 80 ± 5 °C for a period allowing the constant mass to be obtained. The water porosity was calculated using the following relation:

| $$n\,(\%) = \frac{M_{sat} - M_{dry}}{M_{sat} - M_{wat}}$$ | Equation 4 |

with M_{sat} is the mass of the saturated sample, M_{dry} is the mass of the dried sample, and M_{wat} is the mass of the saturated sample immersed in water.

The flexural strength tests were carried out according to the NF EN 1015-11/A1 standard (NF EN 1015-11/A1, 2007) under three-point loading conditions of prismatic specimens up to failure. Prisms with dimensions of 160 mm x 40 mm x 40 mm were prepared in metal moulds, demoulded after 24 hours and then placed in water at room temperature for 28 days before being removed from the water and tested. The compressive strength tests were carried out according to the NF EN 1015-11/A1 standard (NF EN 1015-11/A1, 2007) on the two halves of each prism resulting from the flexural strength tests. Flexural tests were conducted by means of an INSTRON press with a capacity of 100 KN by applying increasing load at a rate of 50 ± 10 N/s until failure. The compression tests were carried out using a servo-hydraulic INSTRON model SCHENCK press with a capacity of 3000 kN by imposing a loading rate of 2400 ± 200 N/s.

The dynamic modulus of elasticity (E_d) was determined according to the standard NF EN ISO 12680-1 (NF EN ISO 12680-1, 2007). Measurements were performed using an ultrasonic testing device E-Metre MK II manufactured by James Instruments based on the resonance frequency measurement.

The total shrinkage measurement was carried out on three 4x4x16 cm of each mortar according to standard NF P 15-433 (NF P 15-433, 1994). The tests started 24 hours after casting and were continued for 28 days.

Using a scanning electron microscope of the LEICA S430i type in backscattered electron mode at a voltage of around 20KV, observations were done on samples measuring 2x2x1.5 cm that were cut from original specimens. The samples were sliced with an abrasive, cleaned and dried before being put into plastic moulds (diameter: 4 cm; height: 3 cm), which were then filled with epoxy resin. The samples were air-dried for 48 hours before testing in order to remove any air that may have remained in the resin. The samples were then polished to provide a smooth surface after demoulding. Making the samples conductive with a Polaron SC502 metallizer and a gold target is the final step before SEM deposition.

3. Experimental results

3.1. Fresh state properties

The rheological characteristics listed in Table 5 are the mean over three measurements plus the standard deviation. For mortars made with recycled sands, a very slight increase in air content (less than 1.5 percent) is observed due to the lower compactness of the recycled sand (Ghorbel et al., 2019).

Note: The table layout displayed in 'Edit' view is not how it will appear in the printed/pdf version. This html display is to enable content corrections to the table. To preview the printed/pdf presentation of the table, please view the 'PDF' tab.

Table 5. Rheological properties of studied mortars. ⊕

| Mixture | Air content (%) | Slump flow after 60 min | | Setting time | | Cone of Marsh based properties | | |
		Slump (mm)	Flow (mm)	Start time (min)	End time (min)	Flow time (s)	Yield stress, τ_0 (Pa)	Viscosity, μ_0 (Pa.s)
M-NS	1.5 ± 0.14	10.7 ± 0.6	20.5 ± 0.7	252	310	54.3 ± 2	17.7 ± 7.2	6.1
M-RS-0	1.6 ± 0.10	7.1 ± 0.7	14.5 ± 0.7	250	280	68.3 ± 4	25.6 ± 7.5	11.2
M-RS-I	2.3 ± 0.07	9.5 ± 0.7	15.5 ± 0.5	257	300	77.0 ± 3	22.3 ± 7.3	11.0
M-RS-II	2.4 ± 0.14	8.1 ± 0.5	13.0 ± 1.0	265	310	66.6 ± 1	21.1 ± 5.9	9.0
M-RS-III	2.7 ± 0.14	11.3 ± 0.8	18.0 ± 0.5	265	310	68.6 ± 1	25.3 ± 6.7	11.1
M-RS-IV	1.9 ± 0.14	11.7 ± 0.5	20.0 ± 0.1	270	310	65 ± 4	14.5 ± 3.3	6.0

Place the cursor position on table column and click 'Add New' to add table footnote.

Figure 4 represents the evolution of the flow and the slump over time during 120 min after mixing. The loss of flow over time is faster for mortars with 10% of recycled sand compared to the reference mortar (Figure 4a and Table 4). The most important flow loss is recorded for the mortar M-RS-0. Moreover, the mortar M-RS-IV presented loss kinetics comparable to that of the reference mortar M-NS while the other mortars show a similar behaviour. Regarding the slump loss over time, it is quite similar to the evolution of the flow as illustrated in Figure 4b and reported in Table 4. The mortar M-RS-IV which has the least accentuated workability loss is the mortar which has the most delayed setting start time. Moreover, the mortar M-RS-0 which loses quickly its workability has the shortest setting start time.

Figure 4. (a) Evolution of mortars flow over time and (b) evolution of mortars slump over time. ⊕
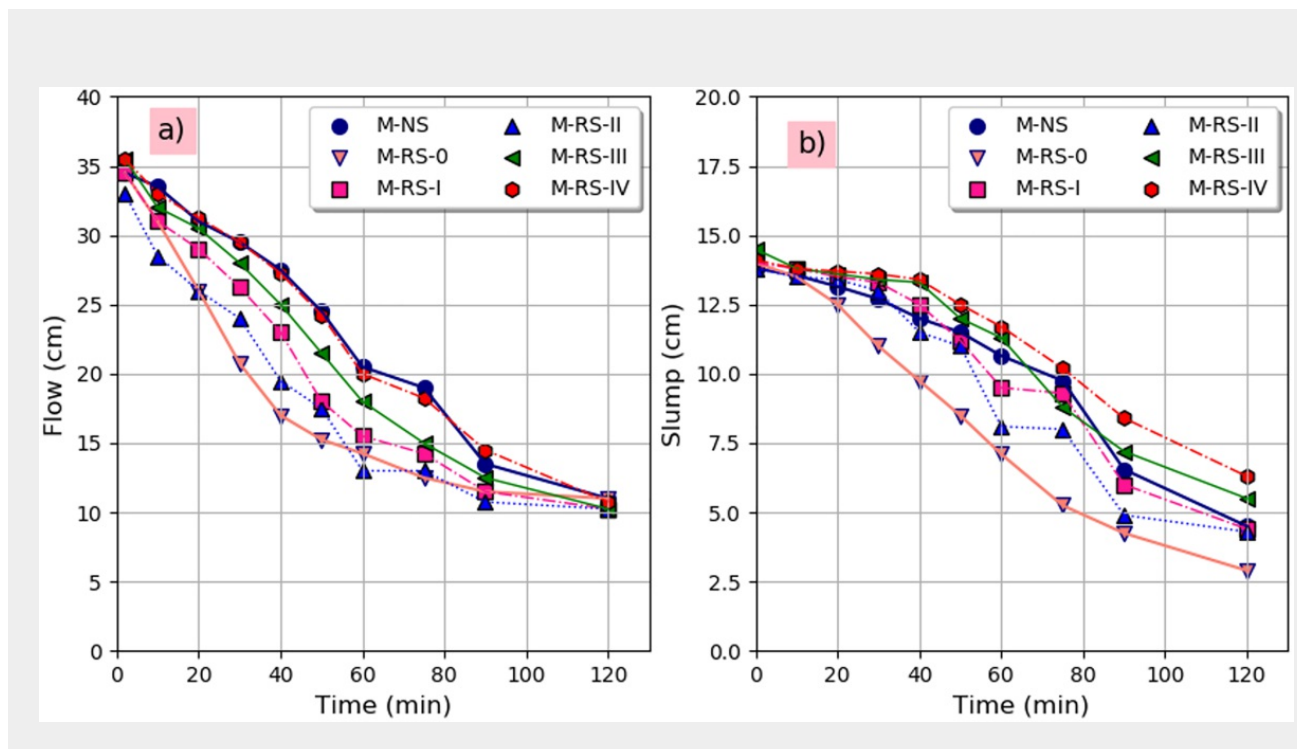
When the total water is held constant, recycled sand continues to absorb the free water present in the mixture, reducing the workability, according to Thang Le et al. (2016). Due to the differences in morphology and particle size between natural and recycled sand with a rough texture, these variations exist in terms of fresh-state behaviour (Berredjem et al., 2018). The higher surface area and water absorption of recycled materials, increase the need for water and result in a faster loss of workability, according to Tran et al. (2021).

The results illustrated in Figure 5 show that the air content increases with the increase in the sand fineness (Figure 5a) as well as the increase in the percentage of fines (Figure 5b). It is worthy to note that a high fineness modulus means that the sand contains an important volume of coarse elements.

Figure 5. (a) Air content versus fineness modulus and (b) Water absorption versus percentage of fines lower than 63 μm). ⊕
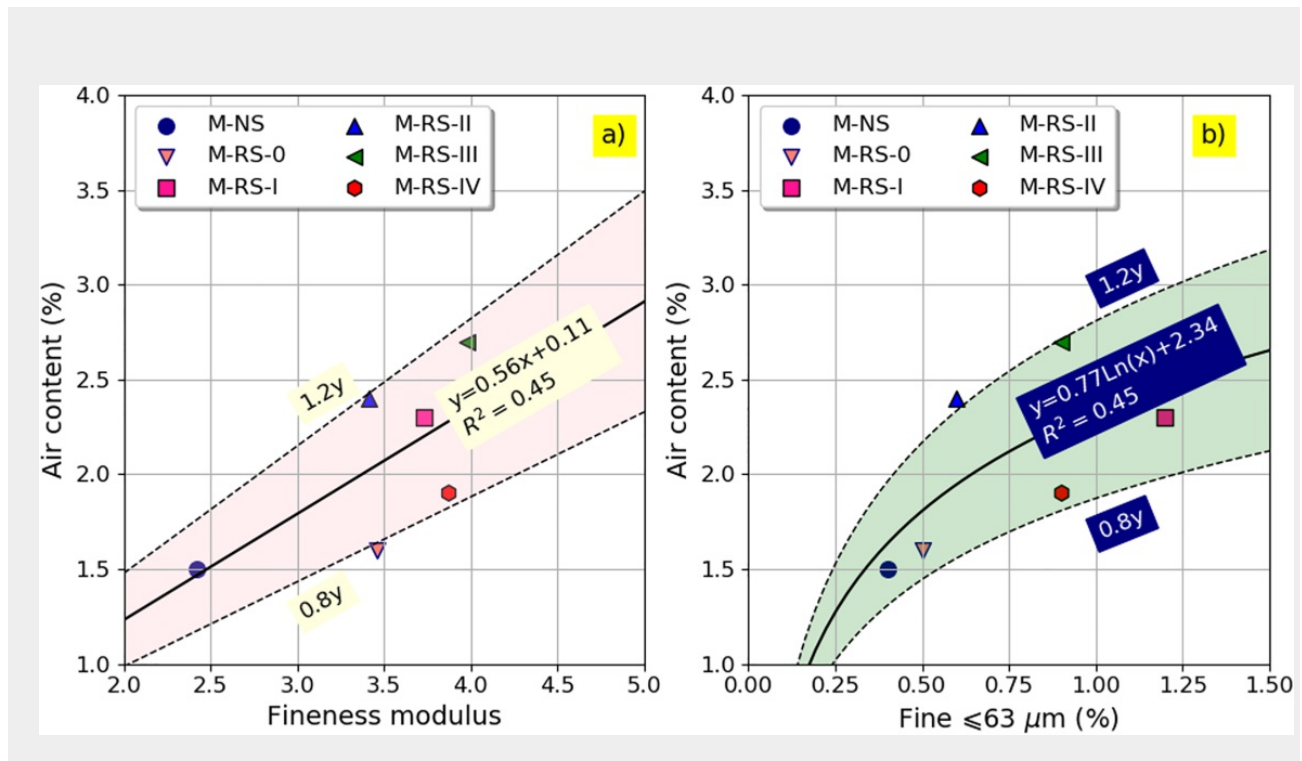
The results recapitulated in Table 4 and illustrated in Figure 6b and 6c show that mortars M-RS-0, M-RS-I, M-RS-II and M-RS-III possess a higher yield stress than M-SN while mortars M-RS-IV have a lower yield stress as compared to M-NS. In terms of viscosity, mortars M-RS-0, M-RS-I and M-RS-III possess higher viscosity than M-SN.

Figure 6. (a) Flow time, (b) yield stress, and (c) viscosity. ⊕
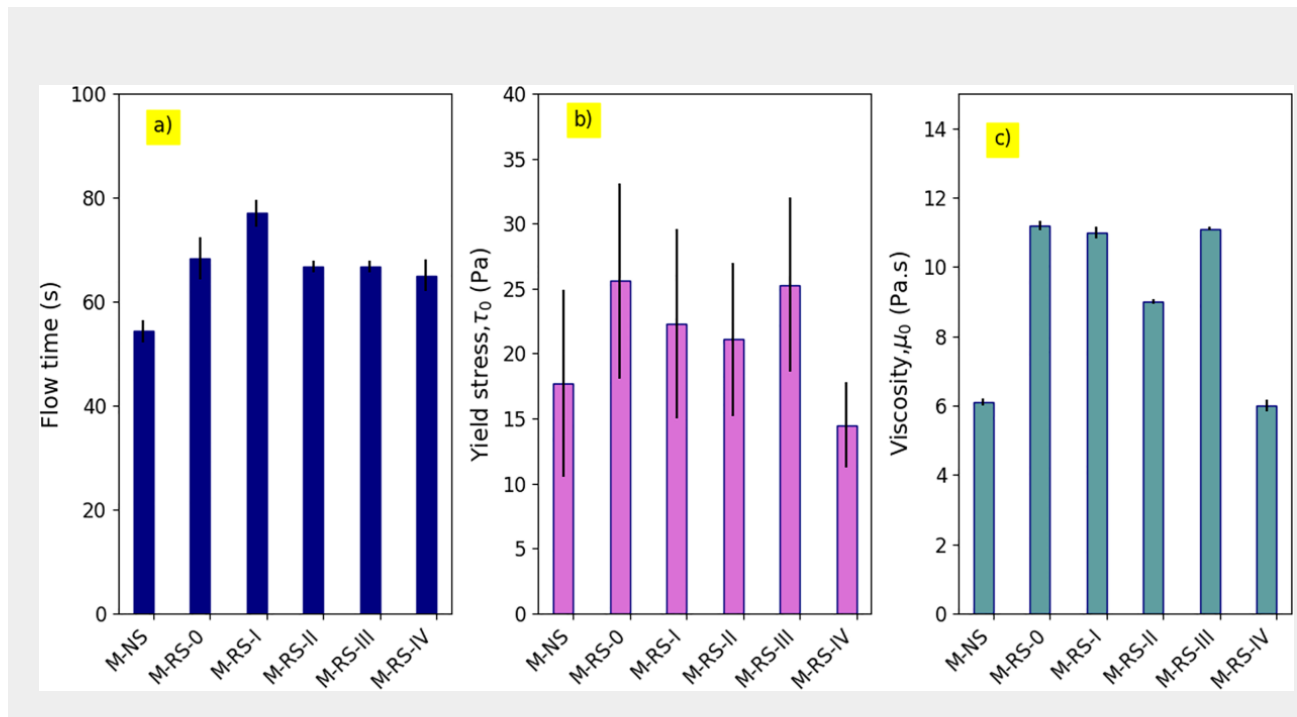
The relationship between rheological properties and air content is depicted in Figure 7. From Figure 7a, it can be shown that the yield stress increases with the air content except for mortar M-RS-V. Similarly, the viscosity increases when the air content increases except for M-RS-V also (Figure 7b). These results, despite the dispersion, are in agreement with the statements of Struble and Jiang (2004) who interpreted this phenomenon by two actions which are the formation of bubble bridges which leads to the increase in the yield stress and the fluid effect of bubbles which leads to the increase in the viscosity. As the air content depends on the fineness modulus (Figure 4), so the rheological properties depend on it too as shown in Figures 7c and 7d.

Figure 7. Rheological parameters versus air content. ⊕
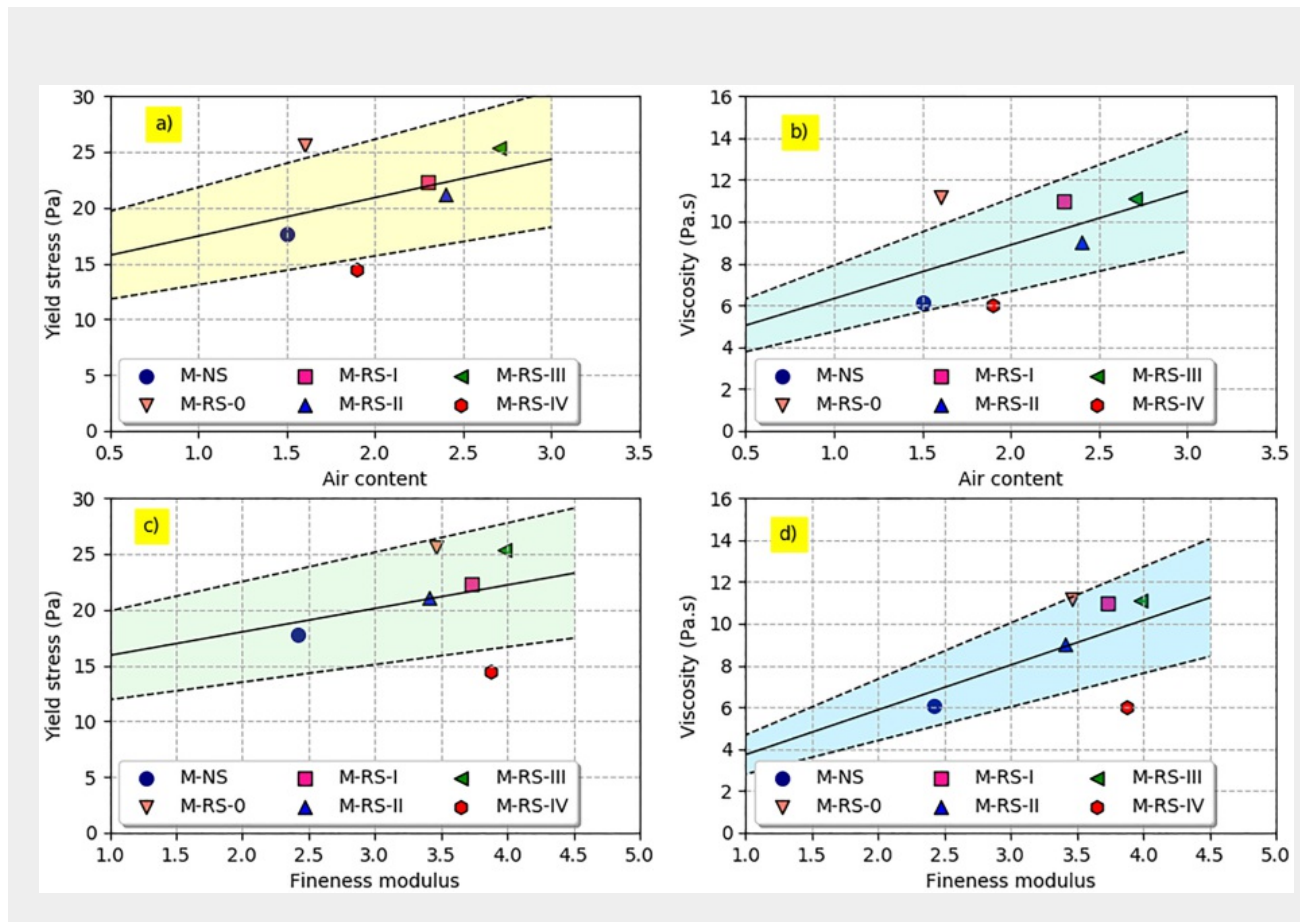
The evolution of the temperature during the hydration process is illustrated in Figure 8a where a maximum temperature of about 50 °C is reached for all mortar specimens after 18 hours followed by a decrease to 23 °C after a period of 100 hours. It can be noticed from Figure 8b that the 10% incorporation of the different types of recycled sand does not affect significantly the hydration process.

Figure 8. (a) Temperature evolution and (b) heat evolution. ⊕
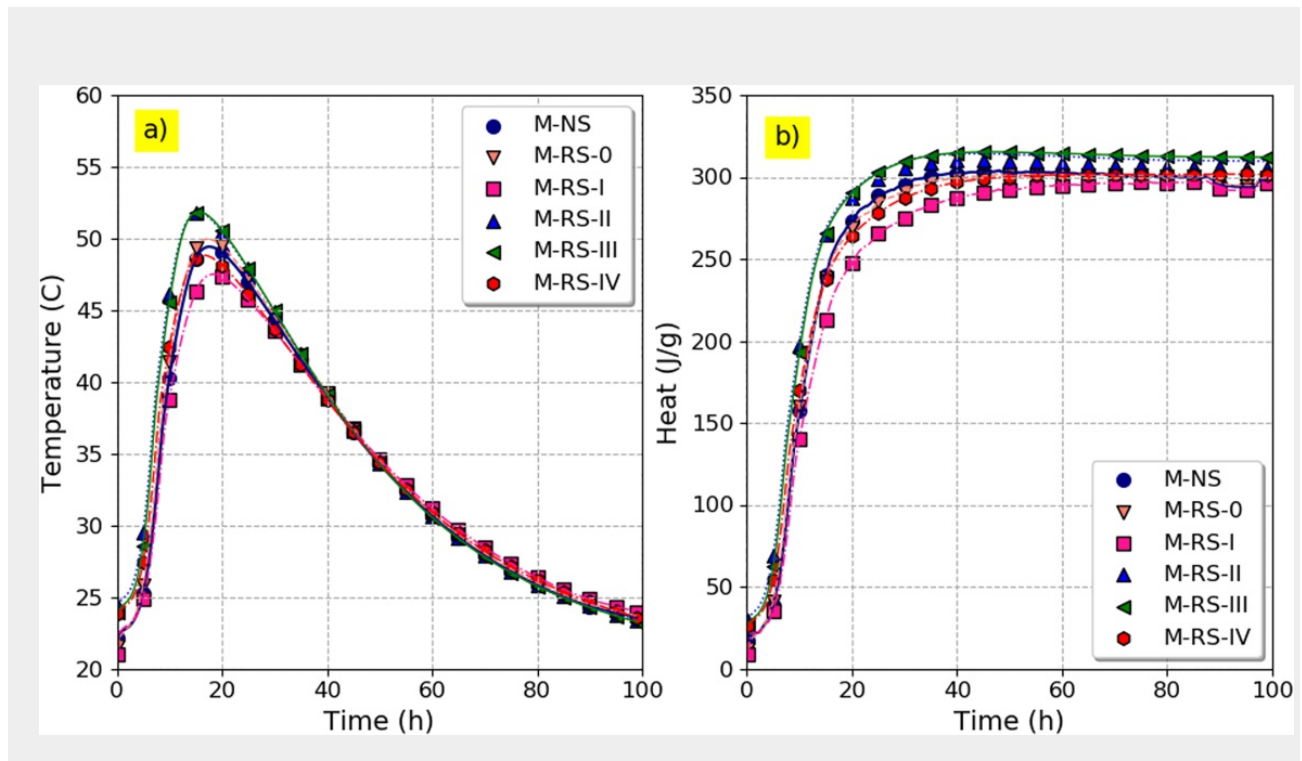
3.2. Physical properties of mortars

The obtained results on the hardened state density and the water porosity are depicted in Figure 9. It can be noticed that the incorporation of 10% recycled sand leads to a slight decrease in the density except for mortar M-RS-IV (Figure 9a). The most significant decrease, recorded for mortar M-RS-0, does not exceed 0.7%, which is the same percentage of the density increase of M-RS-IV.

Figure 9. (a) Density and (b) Water porosity of tested mortars. ⊕
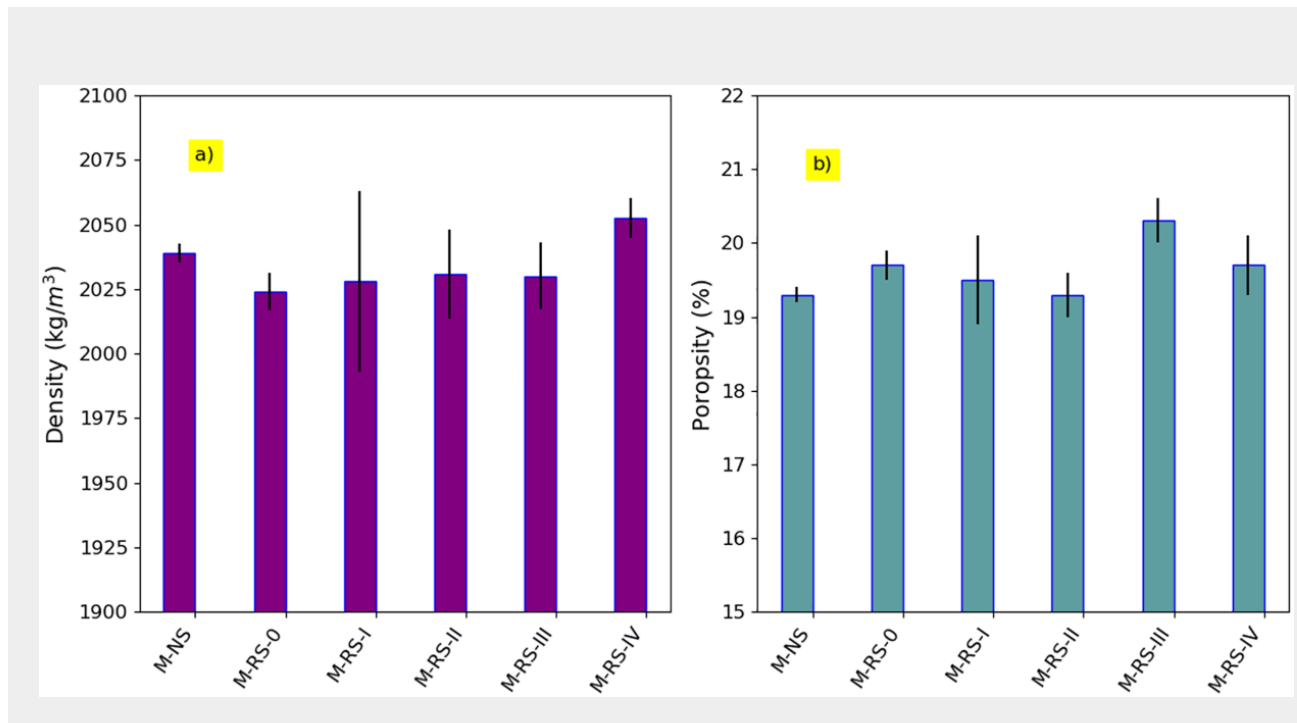
Concerning the porosity, a slight increase can be observed in the Figure 9b except for the mortar M-RS-III which possesses the same porosity as M-NS. The most important porosity, recorded for mortar M-RS-III, is 5.2% higher than the porosity of M-NS.

The SEM observations carried out on the various mortars showed that the interface between the recycled sand and the cement matrix is of good quality (Figure 10). According to Makul et al. (2021), the micro-pores in the old attached mortar can contribute to retaining additional quantities of water and recycled sand behaves as an internal curing agent, which improves the interfacial transition zone (ITZ) between sand particles and the surrounding cement paste. Zhao et al. (2015) claimed also that the saturation state of the cement paste present in the fine recycled aggregates has an impact on the ITZ. When fine recycled aggregates are saturated, water transfers from the surface of the old paste to the new paste, raising the W/C ratio locally at the aggregate's surface and resulting in a wide ITZ. The ITZ for cementitious materials incorporating recycled fines is more cohesive than the ITZ for natural aggregate materials when the fines are pre-saturated, as was also discovered by Evangelista and de Brito (2007).

Figure 10. SEM pictures for developed mortars. ⊕

a) M-NS   b) M-RS-0   c) M-RS-II   d) M-RS-IV
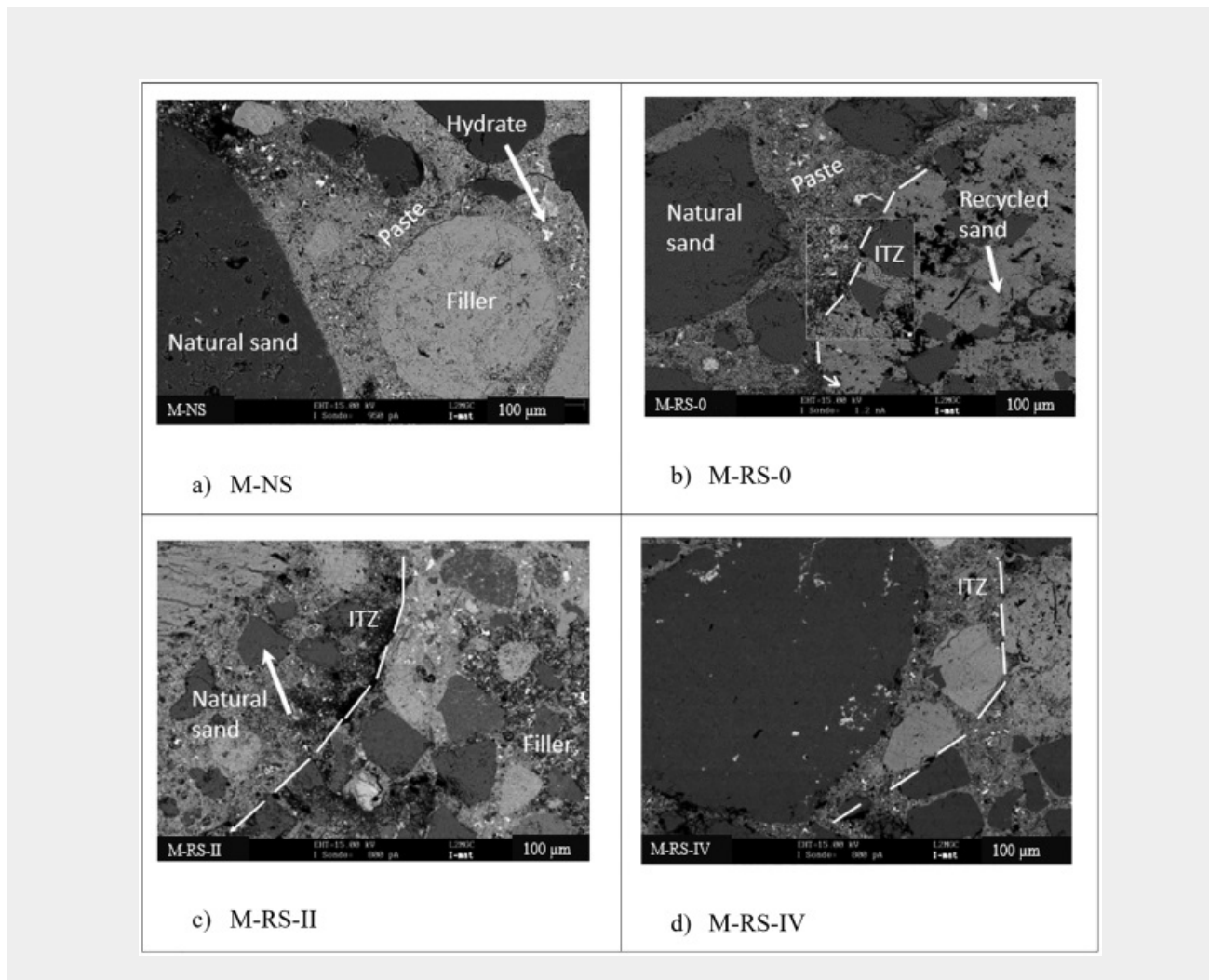
3.3. Mechanical properties of hardened mortars

The results of the mechanical tests, which were performed at 3, 7, 14, 21 and 28 days, are averages with standard deviations. The development of the compressive strengths (f_{cm}) of mortars with time is presented in Figure 11a. The results show that the substitution of 10% of natural sand by recycled sands leads to a reduction in the compressive strengths, but the results remain comparable. Without any abnormalities, the strengths gradually increase over time, with the 3 days strength for all mortars being 60% of the 28 days strength and roughly 95% of the 28 day strength. The M-SR-III mortar, which has the lowest compressive strength at 28 days and the highest porosity due to its higher air content, achieves this result with a reduction in 16% from the M-NS mortar.

Figure 11. Mechanical properties (a) compressive strength and (b) flexural strength. ⊕
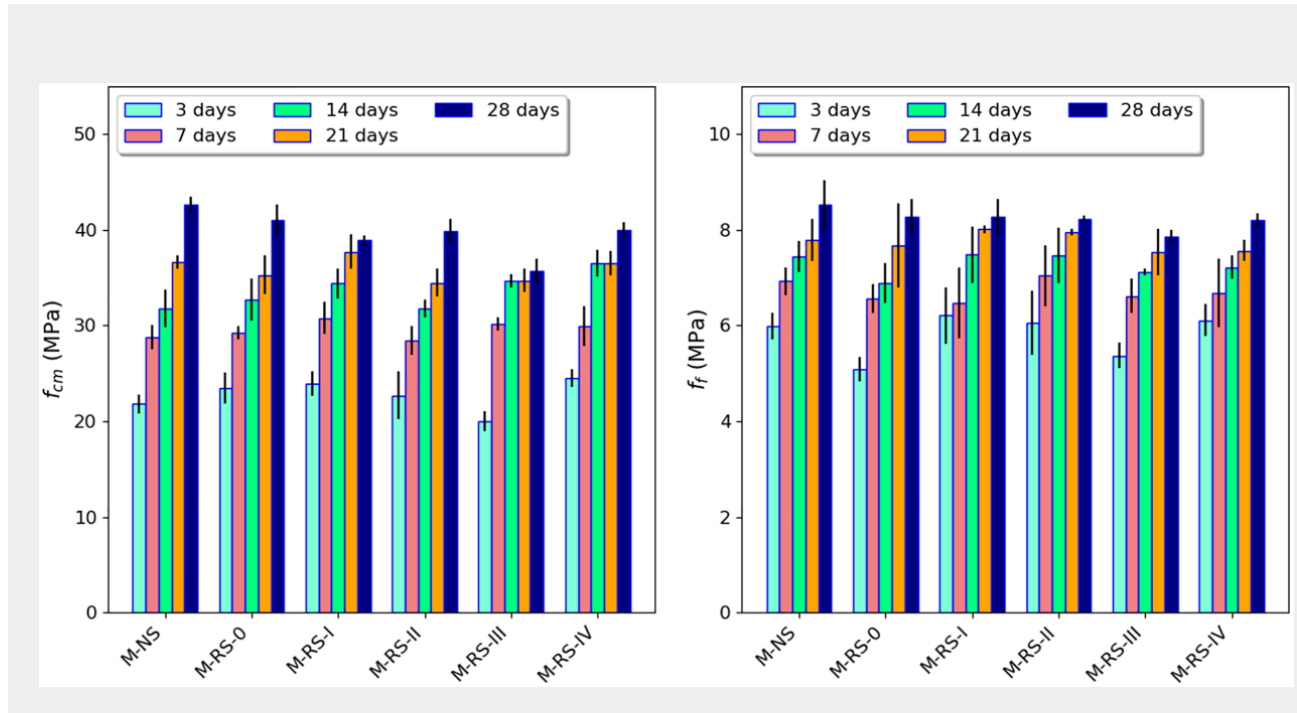
The results presented in Figure 11b show that the flexural strength changes with the age of mortars. The substitution of natural sand with 10% of recycled sand induces an insignificant decrease in the flexural strength at the age of 28 days. The lowest resistance is obtained for M-SR-III mortar with a reduction in 8% as compared to M-NS. The results of the mechanical properties agree with those of Zhao et al. (2015), Ghorbel et al. (2019) and Kou and Poon (2009) who found that recycled sand is harmful in terms of strength.

The evolution of the dynamic modulus of elasticity for all mortars is illustrated in Figure 12 where it can be observed that the substitution of natural sand by 10% of recycled sands does not significantly affect the elastic modulus. A slight decrease, however, is recorded for mortar M-RS-II with a reduction in 4% only.

Figure 12. Evolution of dynamic modulus of elasticity with time. ⊕
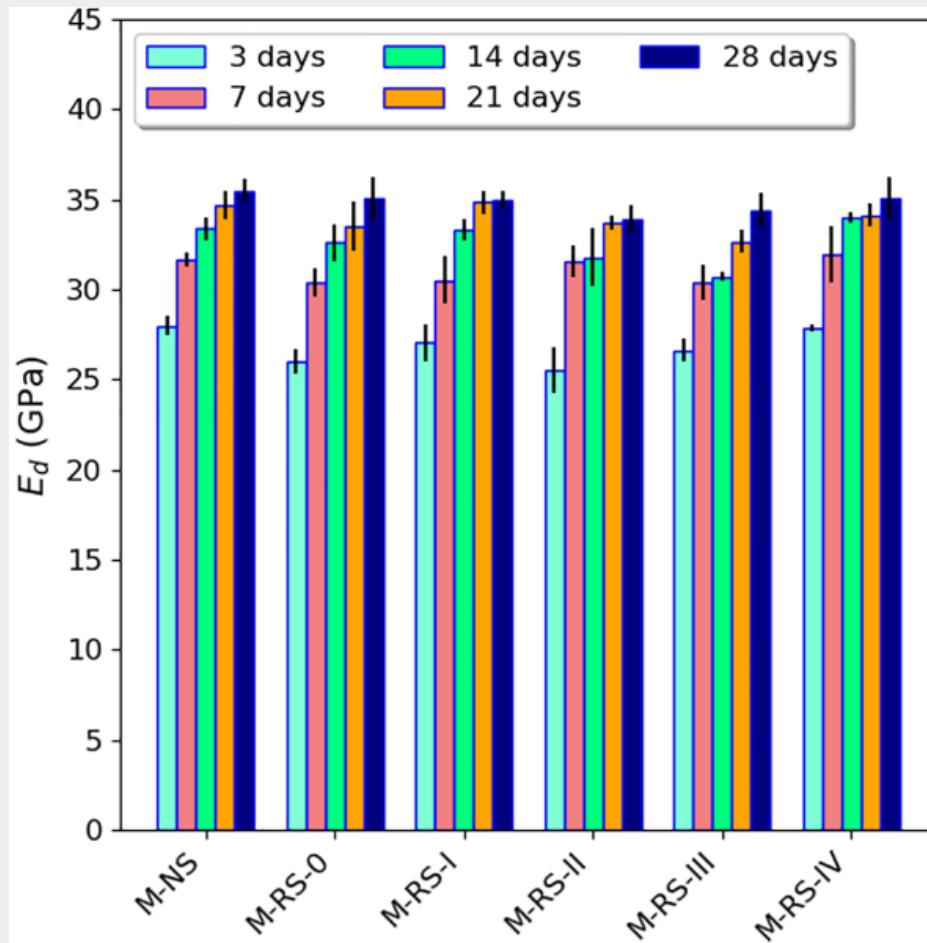
3.4. Shrinkage

The experimental results of total shrinkage are depicted in Figure 13a. It appears that at a young age the mortar M-SR-IV is subject to an important shrinkage compared to other mortars. At 28 days, certain mortars with recycled sands (M-SR-I, M-SR-II and M-SR-III) have a lower shrinkage strain than mortar with natural sand, M-NS.

Figure 13. (a) Experimental shrinkage, and (b) proposed model. ⊕
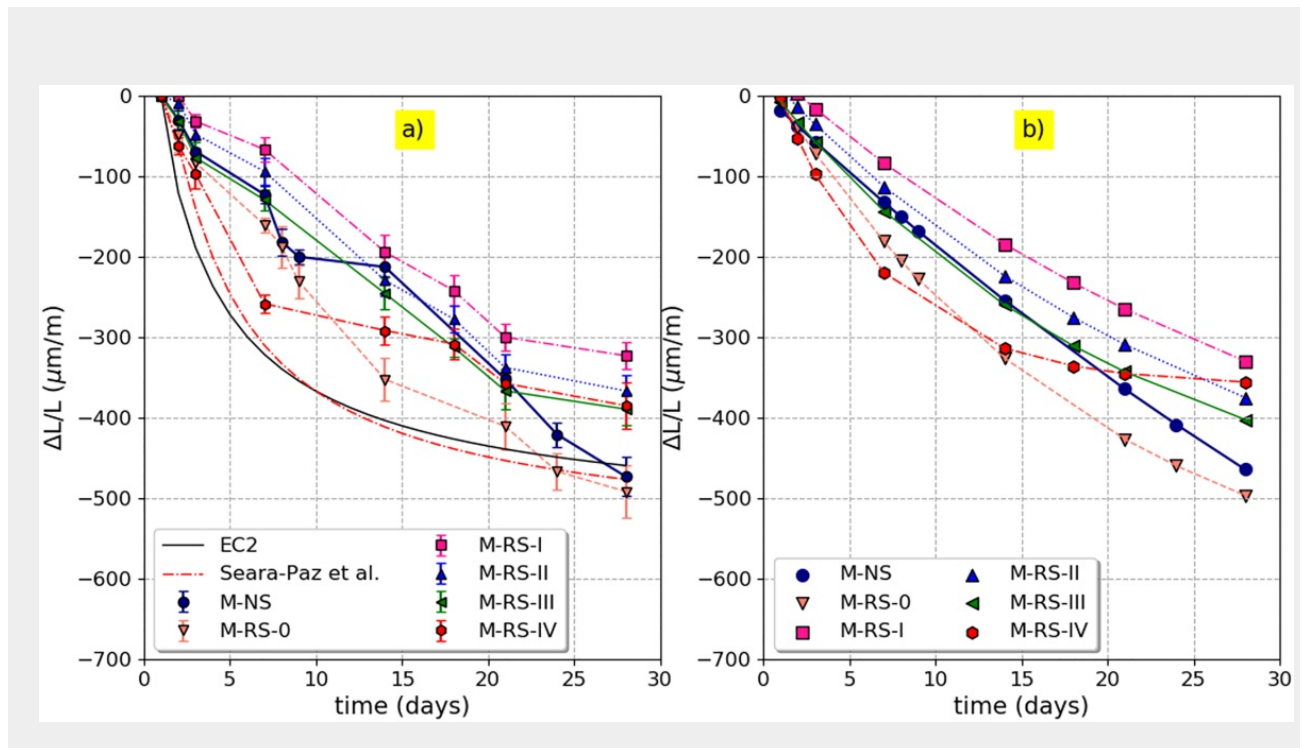
According to EC2 (Comité Européen de Normalisation, 2004) the total shrinkage, named ε_{cs}, consists of two contribution, the first is the autogenous shrinkage, ε_{ca}, and the second is the shrinkage due to drying called ε_{cd}. The development of autogenous shrinkage with time can be expressed as a function of the characteristic compressive strength, f_{ck}, as follows (Comité Européen de Normalisation, 2004):

$\varepsilon_{ca}(t) = \beta_{as}(t) \cdot \varepsilon_{ca}(\infty)$	Equation 5

where

$\varepsilon_{ca}(\infty) = 2.5\,(f_{ck} - 10)\,.10^{-6}$	

$\beta_{as}(t) = 1 - e^{-0.2\sqrt{t}}$ with t, the time taken in days.

The evolution of the drying shrinkage strain over time follows the following expression:

$\varepsilon_{cd}(t) = \beta_{ds}(t, t_s) \cdot k_h \cdot \varepsilon_{cd,0}$	Equation 6

where

t is the time in days.

k_h is a coefficient depending on the size of the element

$$\beta_{ds}(t, t_s) = \frac{(t - t_s)}{(t - t_s) + 0.04\sqrt{h_0^3 3}}$$ Equation 7

t_s is the age of concrete at the end of curing

h_0 is the notional size of the cross section in mm

The basic drying shrinkage can be calculated following to the Eq. 8.

$$\varepsilon_{cd,0} = 0.85\left[(220 + 110.\alpha_{ds1}).e^{\left(-\alpha_{ds2}\frac{f_{cm}}{10}\right)}\right].10^{-6}\beta_{RH}$$ Equation 8

$$\beta_{RH} = 1.55\left[1 - \left(\frac{RH}{100}\right)^3\right]$$ Equation 9

with α_{ds1} and α_{ds2} two parameters which depend on the cement type.

The total shrinkage was estimated according to the analytical model of EC2 based on the characteristics of the reference mortar M-NS and the results are depicted in Figure 13a with the experimental results. It can be shown that EC2 overestimates the shrinkage at early age but at 28 days the prediction is comparable to the experimental results. The least important shrinkage strain is shown by the mortar M-RS-I which represents 70% of the strain shown by M-NS. Sear-Paz el al. (Seara-Paz et al., 2016) proposed to modify the value predicted by the standard by introducing the two $\left(1 + 0.44RCA\right)\left(e^{0.01RCA\left[1 - \left(\frac{90}{t}\right)^{(1.82-1.04RCA)}\right]}\right)$ with RCA the percentage of recycled aggregates. The modified curve depicted in Figure 13a shows that this modification is not sufficient to model the experimental results.

Based on the obtained results, the following equation is proposed to model the total shrinkage strain:

$$\frac{\Delta L}{L}\left(\frac{\mu m}{m}\right) = ae^{-bt} + c$$ Equation 10

Indeed, a and b influence the kinematics of the shrinkage strain while c represents the final value when time tends towards infinity.

The parameters a, b and c were optimised by minimising the differences between the experimental and predicted values (Figure 13b). It can be noticed form values regrouped in Table 6 that mortars M-RS-I and M-RS-II behave similarly. The evolution of shrinkage strain at the age of 28 days as a function of the

percentage of fines is represented in Figure 14a. In view of the obtained results, it can be concluded that the strain decreases with the increase in the percentage of fines whose diameter is lower than 63 μm. Similarly, the parameter C in Equation 11 which represents the final shrinkage value when the time dtends to infinity is shown in Figure 14b. **AQ2** As the fines content increases, there will likely be fewer micropores and therefore less tensile stress inducing shrinkage.

Figure 14. (a) Shrinkage strain versus the percentage of fines lower than 63 μm at 28 days and (b) the final predicted strain. ➕
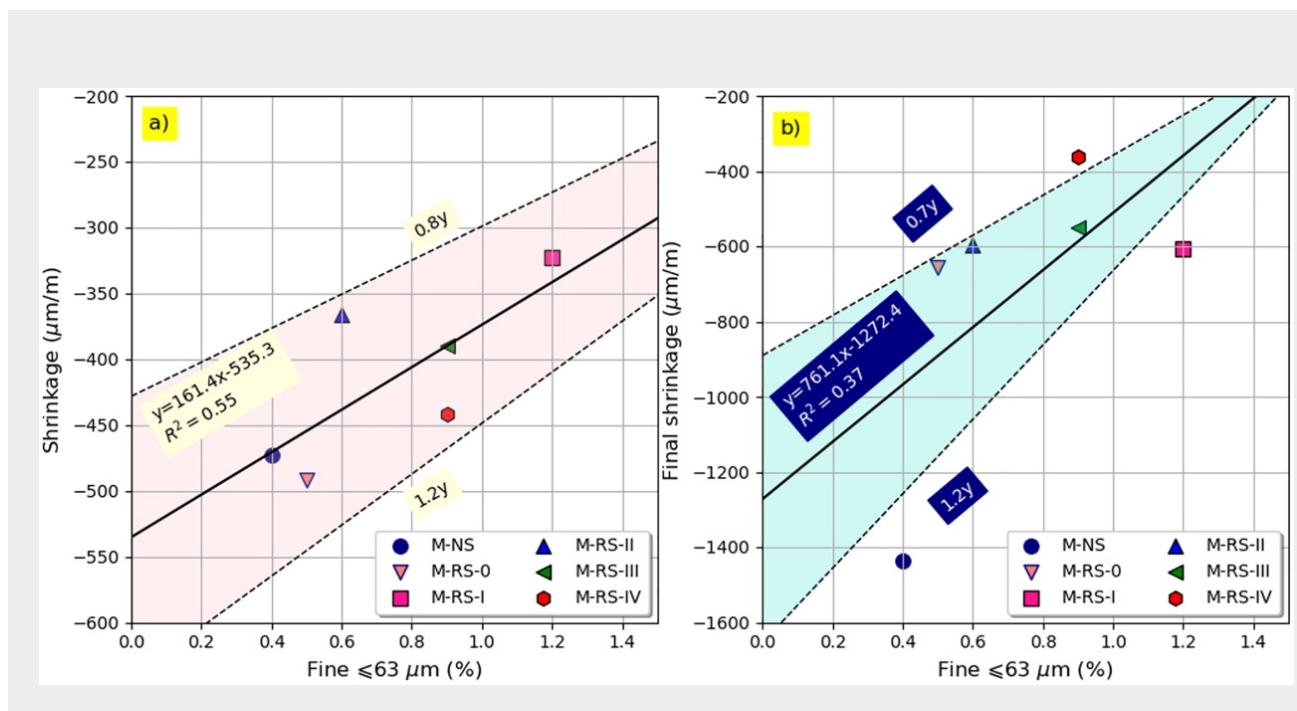
Note: The table layout displayed in 'Edit' view is not how it will appear in the printed/pdf version. This html display is to enable content corrections to the table. To preview the printed/pdf presentation of the table, please view the 'PDF' tab.

Table 6. Fitting parameters of the proposed model. ➕

Mortar	a	b	c	R²
M-NS	1438.0	0.014	−1436.0	0.96

M-RS-0	683.6	0.052	−656.0	0.93
M-RS-I	638.9	0.031	−607.0	0.93
M-RS-II	628.6	0.037	−598.1	0.95
M-RS-III	570.7	0.048	−551.2	0.96
M-RS-IV	420.8	0.156	−361.1	0.89

Place the cursor position on table column and click 'Add New' to add table footnote.

3.5. Discussion

In order to estimate the effect of the incorporation of recycled the relative variation in each property, named V, was calculated such that:

$$V = \frac{P^{M-RS-i} - P^{M-NS}}{P^{M-NS}} \times 100$$

Equation 11

where P^{M-RS-i} is the studied property of the recycled sand i and P^{M-NS} is the equivalent property of the natural sand. Hence, positive values indicate an increase in the evaluated property.

In general, the addition of 10% recycled sand affects the workability after mixing (Figures 15a and 15b). The mortar M-RS-III, with the highest viscosity (Figure 15b), displays a slump that is higher than that of M-SN (Figure 15a). The variation in the slump and flow at the fresh condition is greatly influenced by the different morphology and texture of the used sands. Compared to rolled natural sand, recycled sand may have coarse particles and a rough texture which lead to a decrease in the slump and flow. However, when the texture is the same, these characteristics do not differ between recycled sand mortars and natural sand mortars.

Figure 15. Properties variation in fresh and hardened states. ➕

a)

b)

c)

d)
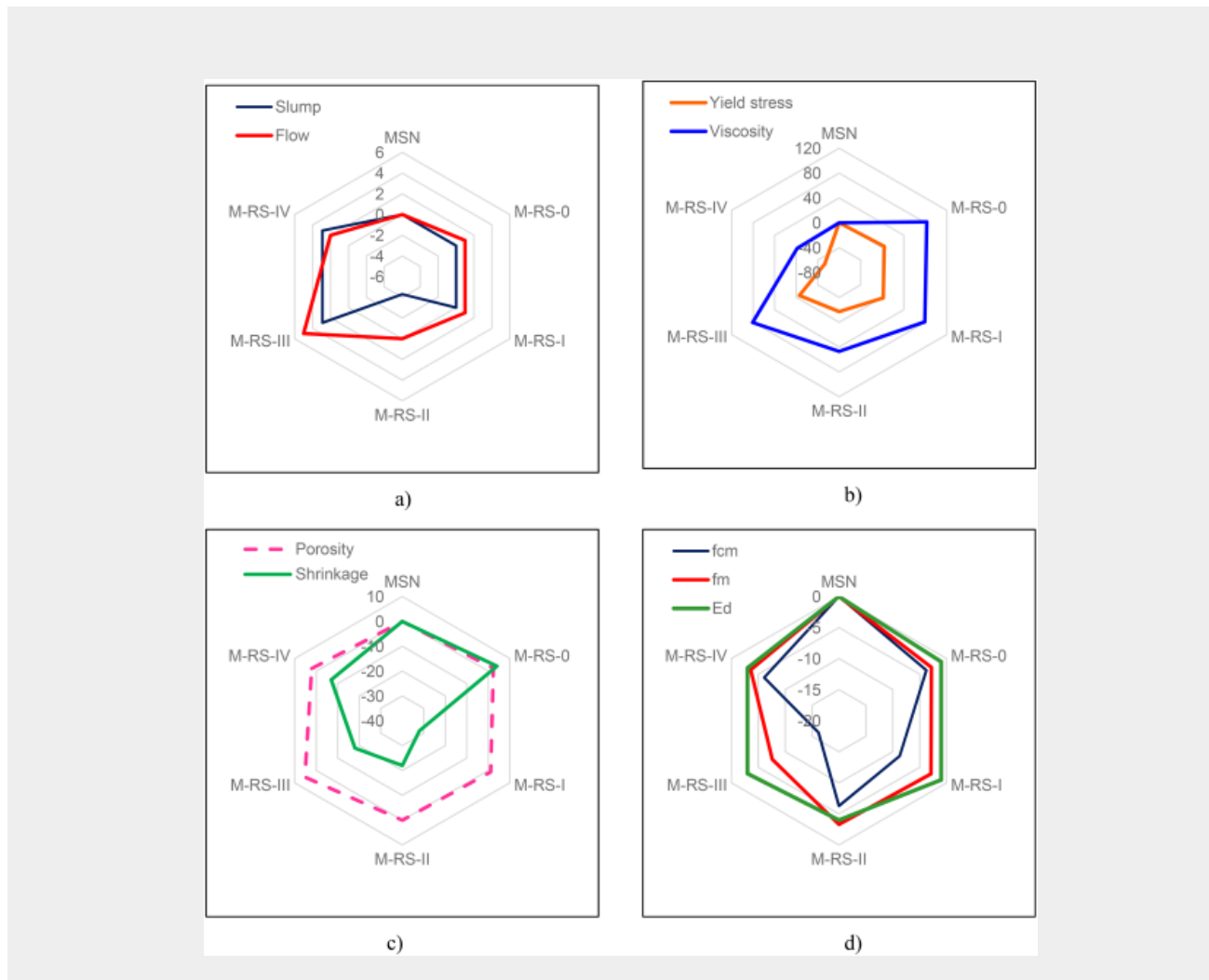
From the results obtained, it can be also concluded that the introduction of 10% recycled sand in mortar mixtures does not significantly affect the mechanical properties at 28 days regardless of its nature and origin (Figure 15c). Based on Figures 15c and 15d, the mortar M-RS-III presented a lowest compressive strength due to its higher porosity.

4. Conclusions

The research described in this article was carried out to assess how the variety of recycled sands affects the characteristics of mortars. In order to accomplish this, an experimental program was established to investigate the properties of concrete mortars in both their fresh and hardened states, in which five different types of recycled sand were used to replace 10% of the natural sand.

Using the equivalent concrete mortar approach, the composition of the mortars was derived from a natural

aggregate concrete mixture with a C35/45 strength class. The cement and filler contents, the effective water to the cement ratio and the superplasticizer dosage were all held constant for all the developed mortars.

Recycled sand was discovered to have an impact on the properties of mortar. Compared to natural sand mortar, the air content rises and the increased yield stress and plastic viscosity are the results of this increase. When recycled sand is utilised, the flow loss is more pronounced. Compared to natural sand mortar, some mortars demonstrated a slower loss throughout the evolution of the slump over time.

The porosity and water absorption capacity of mortars made using recycled sands are generally increased. The highest results for the mortar M-RS-III were 6% and 5%, respectively. In terms of mechanical properties, the compressive strength of all recycled sand mortars is less than the strength of the reference mortar M-NS. The mortar M-RS-III achieved also the lowest result for compressive and flexural strengths at the age of 28 days due to its highest porosity and air content in the fresh state, with a reduction in 16.2% in compressive strength and 8% in terms of flexural strength. The substitution of natural sand by 10% of recycled sand does not significantly affect the elastic modulus. A slight decrease was recorded for mortar M-RS-II with only 4% reduction. Finally, the total shrinkage decreases as the fines content increases.

In conclusion, attention should be given to a reduction in the mechanical properties and deterioration of the state's properties if recycled sand is introduced at a low dosage to mortar.

Disclosure statement

No potential conflict of interest was reported by the authors. AQ3

Data availability statement

The data that support the findings of this study are available from the corresponding author Elhem Ghorbel upon reasonable request.

> **Note:** this Edit/html view does not display references as per your journal style. There is no need to correct this. The content is correct and it will be converted to your journal style in the published version.

References

Bao, Z., Lu, W., Chi, B., Yuan, H., & Hao, J. (2019). Procurement innovation for a circular economy of construction and demolition waste: Lessons learnt from Suzhou, China. *Waste management (New York, N.Y.)*, *99*, 12–21. https://doi.org/10.1016/j.wasman.2019.08.031

Bouvet, A., Ghorbel, E., & Bennacer, R. (2010). The mini-conical slump flow test: Analysis and numerical study. *Cement and Concrete Research*, *40*(10), 1517–1523. https://doi.org/10.1016/j.cemconres.2010.06.005

➕ ✏️ 🗑️

Braga, M., de Brito, J., & Veiga, R. (2012). Incorporation of fine concrete aggregates in mortars. *Construction and Building Materials*, *36*, 960–968. https://doi.org/10.1016/j.conbuildmat.2012.06.031 ➕ ✏️ 🗑️

BS EN 459-2. (2010). Building lime. Test methods. ➕ ✏️ 🗑️

Comité Européen de Normalisation. (2004). Eurocode 2. Design of concrete structures – Part 1: Common rules for building and civil engineering structures. ➕ ✏️ 🗑️

Corinaldesi, V., & Moriconi, G. (2009). Influence of mineral additions on the performance of 100% recycled aggregate concrete. *Construction and Building Materials*, *23*(8), 2869–2876. https://doi.org/10.1016/j.conbuildmat.2009.02.004 ➕ ✏️ 🗑️

Corinaldesi, V., & Moriconi, G. (2010). Recycling of rubble from building demolition for low-shrinkage concretes. *Waste management (New York, N.Y.)*, *30*(4), 655–659. https://doi.org/10.1016/j.wasman.2009.11.026 ➕ ✏️ 🗑️

Cuenca-Moyano, G. M., Martín-Morales, M., Valverde-Palacios, I., Valverde-Espinosa, I., & Zamorano, M. (2014). Influence of pre-soaked recycled fine aggregate on the properties of masonry mortar. *Construction and Building Materials*, *70*, 71–79. https://doi.org/10.1016/j.conbuildmat.2014.07.098 ➕ ✏️ 🗑️

de Juan, M. S., & Gutiérrez, P. A. (2009). Study on the influence of attached mortar content on the properties of recycled concrete aggregate. *Construction and Building Materials*, *23*(2), 872–877. https://doi.org/10.1016/j.conbuildmat.2008.04.012 ➕ ✏️ 🗑️

Dapena, E., Alaejos, P., Lobet, A., & Pérez, D. (2011). Effect of recycled sand content on characteristics of mortars and concretes. *Journal of Materials in Civil Engineering*, *23*(4), 414–422. https://doi.org/10.1061/(ASCE)MT.1943-5533.0000183 ➕ ✏️ 🗑️

Ecological Transition Agency. (2020). Building waste. Retrieved from https://www.ademe.fr/ ➕ ✏️ 🗑️

Evangelista, L., & de Brito, J. (2007). Mechanical behaviour of concrete made with fine recycled concrete aggregates. *Cement and Concrete Composites*, *29*(5), 397–401. https://doi.org/10.1016/j.cemconcomp.2006.12.004 ➕ ✏️ 🗑️

Evangelista, L., Guedes, M., de Brito, J., Ferro, A. C., & Pereira, M. F. (2015). Physical, chemical and mineralogical properties of fine recycled aggregates made from concrete waste. *Construction and Building Materials*, *86*, 178–188. https://doi.org/10.1016/j.conbuildmat.2015.03.112 ➕ ✏️ 🗑️

Fořt, J., & Černý, R. (2020). Transition to circular economy in the construction industry: Environmental aspects of waste brick recycling scenarios. *Waste management (New York, N.Y.)*, *118*, 510–520.

https://doi.org/10.1016/j.wasman.2020.09.004

Francois, d L., & Colina, H. (2019). *Concrete recycling: Research and practice* (C. Press. Ed.). **AQ4**

Ghorbel, E., Wardeh, G., & Fares, H. (2019). Mechanical and fracture properties of recycled aggregate concrete in design codes and empirical models. *Structural Concrete*, *20*(6), 2156–2170. https://doi.org/10.1002/suco.201800335

Ghorbel, E., Wardeh, G., Gomart, H., & Matar, P. (2020). Formulation parameters effects on the performances of concrete equivalent mortars incorporating different ratios of recycled sand. *Journal of Building Physics*, *43*(6), 545–572. https://doi.org/10.1177/1744259119896093 **AQ5**

Ginga, C. P., Ongpeng, J. M. C., & Daly, M. K. M. (2020). Circular economy on construction and demolition waste: A literature review on material recovery and production. *Materials*, *13*(13), 2970. https://doi.org/10.3390/ma13132970

González-Fonteboa, B., Martínez-Abella, F., Herrador, M. F., & Seara-Paz, S. (2012). Structural recycled concrete: Behaviour under low loading rate. *Construction and Building Materials*, *28*(1), 111–116. https://doi.org/10.1016/j.conbuildmat.2011.08.010

Haeusler, L., & Berthoin, G. (2015). Déchets. Edition 2015. Retrieved from http://www.ademe.fr/

Struble, L. J., & Jiang, Q. (2004). Effects of air entrainment on rheology. *ACI Materials Journal*, *101*(6). https://doi.org/10.14359/13483 **AQ6**

Kim, J. (2021). Properties of recycled aggregate concrete designed with equivalent mortar volume mix design. *Construction and Building Materials*, *301*, 124091. https://doi.org/10.1016/j.conbuildmat.2021.124091

Kou, S. C., & Poon, C. S. (2009). Properties of self-compacting concrete prepared with coarse and fine recycled concrete aggregates. *Cement and Concrete Composites*, *31*(9), 622–627. https://doi.org/10.1016/j.cemconcomp.2009.06.005

Berredjem, L., Arabi, N., Molez, L., & B, J. (2018). Influence of recycled sand containing fillers on the rheological and mechanical properties of masonry mortars. *Journal of Materials and Environmental Science*, *9*(4), 1255–1265.

Le, T., Rémond, S., Le Saout, G., & Garcia-Diaz, E. (2016). Fresh behavior of mortar based on recycled sand—Influence of moisture condition. *Construction and Building Materials*, *106*, 35–42. https://doi.org/10.1016/j.conbuildmat.2015.12.071

Ledesma, E. F., Jiménez, J. R., Ayuso, J., Fernández, J. M., & De Brito, J. (2015). Maximum feasible use

of recycled sand from construction and demolition waste for eco-mortar production—Part-I: Ceramic masonry waste. *Journal of Cleaner Production*, *87*, 692–706. https://doi.org/10.1016/j.jclepro.2014.10.084 ➕ ✏️ 🗑️

Makul, N., Fediuk, R., Amran, M., Zeyad, A. M., Murali, G., Vatin, N., Klyuev, S., Ozbakkaloglu, T., & Vasilev, Y. (2021). Use of recycled concrete aggregates in production of green cement-based concrete composites: A review. *Crystals*, *11*(3), 232. https://doi.org/10.3390/cryst11030232 ➕ ✏️ 🗑️

Mohamed, M. A. S., Ghorbel, E., & Wardeh, G. (2010). Valorization of micro-cellulose fibers in self-compacting concrete. *Construction and Building Materials*, *24*(12), 2473–2480. https://doi.org/10.1016/j.conbuildmat.2010.06.009 ➕ ✏️ 🗑️

NF EN 1015-11/A1. (2007). *Methods of test for mortar for masonry—Part 11: determination of flexural and compressive strength of hardened mortar*. ➕ ✏️ 🗑️

NF EN 1015-6. (1999). *Methods of test for mortar for masonry. Part 6: determination of bulk density of fresh mortar*. ➕ ✏️ 🗑️

NF EN 1015-7. (1999). *Methods of test for mortar for masonry. Part 7: determination of air content of fresh mortar*. ➕ ✏️ 🗑️

NF EN 1097-6. (2014). *Tests for mechanical and physical properties of aggregates—Part 6: determination of particle density and water absorption*. ➕ ✏️ 🗑️

NF EN 1097-7. (2008). *Tests for mechanical and physical properties of aggregates—Part 7: determination of the particle density of filler—Pyknometer method*. ➕ ✏️ 🗑️

NF EN 12350-2. (2010). *Testing fresh concrete—Part 2: slump test*. ➕ ✏️ 🗑️

NF EN 13139. (2003). *Aggregates for mortar*. ➕ ✏️ 🗑️

NF EN 196-1. (2006). *Methods of testing cement*. Determination of strength. ➕ ✏️ 🗑️

NF EN 206-1. (2014). *Concrete—Specification, performance, production and conformity*. ➕ ✏️ 🗑️

NF EN 480-2. (2006). *Admixtures for concrete, mortar and grout—Test methods—Part 2: determination of setting time—Adjuvants pour béton, mortier et coulis*. ➕ ✏️ 🗑️

NF EN 933-1. (2012). *Tests for geometrical properties of aggregates—Part 1: determination of particle size distribution—Sieving method*. ➕ ✏️ 🗑️

NF EN 933-8 + A1. (2015). *Tests for geometrical properties of aggregates—Part 8: assessment of fines—Sand equivalent test*. ➕ ✏️ 🗑️

NF EN ISO 12680-1. (2007). *Methods of test for refractory products—Part 1: determination of dynamic*

Young's modulus (MOE) by impulse excitation of vibration.

NF P 15-433. (1994). *Methods of testing cement. Determination of shrinkage and swelling.*

NF P18-459. (2010). *Concrete—Testing hardened concrete—Testing porosity and density.*

NF P18-507. (1992). *Additions for concrete. Water retention. Method for measurement of fluidity by flowing with the "cone de marsh".*

Omary, S., Ghorbel, E., & Wardeh, G. (2016). Relationships between recycled concrete aggregates characteristics and recycled aggregates concretes properties. *Construction and Building Materials*, *108*, 163–174. https://doi.org/10.1016/j.conbuildmat.2016.01.042

Omary, S., Ghorbel, E., Wardeh, G., & Nguyen, M. D. (2018). Mix design and recycled aggregates effects on the concrete's properties. *International Journal of Civil Engineering*, *16*(8), 973–992. https://doi.org/10.1007/s40999-017-0247-y

Saiz-Martínez, P., González-Cortina, M., & Fernández-Martínez, F. (2015). Characterization and influence of fine recycled aggregates on masonry mortars properties. *Materiales de Construcción*, *65*(319), e058–10. https://doi.org/10.3989/mc.2015.06014

Roussel, N., & Coussot, P. (2005). "Fifty-cent rheometer" for yield stress measurements: From slump to spreading flow. *Journal of Rheology*, *49*(3), 705–718. https://doi.org/10.1122/1.1879041

Sanguino, R., Barroso, A., Fernández-Rodríguez, S., & Sánchez-Hernández, M. I. (2020). Current trends in economy, sustainable development, and energy: A circular economy view. *Environmental science and Pollution Research International*, *27*(1), 1–7. https://doi.org/10.1007/s11356-019-07074-x

Schwartzentruber, A., & Catherine, C. (2000). La méthode du mortier de béton équivalent (MBE)–-Un nouvel outil d'aide à la formulation des bétons adjuvantés. *Materials and Structures*, *33*(8), 475–482. https://doi.org/10.1007/BF02480524

Seara-Paz, S., González-Fonteboa, B., Martínez-Abella, F., & González-Taboada, I. (2016). Time-dependent behaviour of structural concrete made with recycled coarse aggregates. Creep and shrinkage. *Construction and Building Materials*, *122*, 95–109. https://doi.org/10.1016/j.conbuildmat.2016.06.050

Tran, D. V., Allawi, A., Albayati, A., Cao, T. N., El-Zohairy, A., & Nguyen, Y. T. (2021). Recycled concrete aggregate for medium-quality structural concrete. *Materials*, *14*(16), 4612. https://doi.org/10.3390/ma14164612

UNPG. (2015). Union Nationale des Producteurs de Granulats. Retrieved from http://www.unpg.fr

Vegas, I., Azkarate, I., Juarrero, A., & Frías, M. (2009). Design and performance of masonry mortars made

with recycled concrete aggregates. *Materiales de Construcción*, *59*(295), 5–18. https://doi.org/10.3989/mc.2009.44207 ➕ ✏️ 🗑️

Velay-Lizancos, M., Vazquez-Burgo, P., Restrepo, D., & Martinez-Lage, I. (2018). Effect of fine and coarse recycled concrete aggregate on the mechanical behavior of precast reinforced beams: Comparison of FE simulations, theoretical, and experimental results on real scale beams. *Construction and Building Materials*, *191*, 1109–1119. https://doi.org/10.1016/j.conbuildmat.2018.10.075 ➕ ✏️ 🗑️

Wardeh, G., & Ghorbel, E. (2019). Shear strength of reinforced concrete beams with recycled aggregates. *Advances in Structural Engineering*, *22*(8), 1938–1951. https://doi.org/10.1177/1369433219829815 ➕ ✏️ 🗑️

Wardeh, G., Ghorbel, E., & Gomart, H. (2015). Mix design and properties of recycled aggregate concretes: Applicability of Eurocode 2. *International Journal of Concrete Structures and Materials*, *9*(1), 1–20. https://doi.org/10.1007/s40069-014-0087-y ➕ ✏️ 🗑️

Wardeh, G., Ghorbel, E., Gomart, H., & Fiorio, B. (2017). Experimental and analytical study of bond behavior between recycled aggregate concrete and steel bars using a pullout test. *Structural Concrete*, *18*(5), 811–825. https://doi.org/10.1002/suco.201600155 ➕ ✏️ 🗑️

Yu, Y., Yazan, D. M., Bhochhibhoya, S., & Volker, L. (2021). Towards circular economy through industrial symbiosis in the Dutch construction industry: A case of recycled concrete aggregates. *Journal of Cleaner Production*, *293*, 126083. https://doi.org/10.1016/j.jclepro.2021.126083 ➕ ✏️ 🗑️

Zega, C. J., Villagrán-Zaccardi, Y. A., & Di Maio, A. A. (2010). Effect of natural coarse aggregate type on the physical and mechanical properties of recycled coarse aggregates. *Materials and Structures*, *43*(1–2), 195–202. https://doi.org/10.1617/s11527-009-9480-4 ➕ ✏️ 🗑️

Zhang, H., Ji, T., Zeng, X., Yang, Z., Lin, X., & Liang, Y. (2018). Mechanical behavior of ultra-high performance concrete (UHPC) using recycled fine aggregate cured under different conditions and the mechanism based on integrated microstructural parameters. *Construction and Building Materials*, *192*, 489–507. https://doi.org/10.1016/j.conbuildmat.2018.10.117 ➕ ✏️ 🗑️

Zhao, Z., Remond, S., Damidot, D., & Xu, W. (2013). Influence of hardened cement paste content on the water absorption of fine recycled concrete aggregates. *Journal of Sustainable Cement-Based Materials*, *2*(3–4), 186–203. https://doi.org/10.1080/21650373.2013.812942 ➕ ✏️ 🗑️

Zhao, Z., Remond, S., Damidot, D., & Xu, W. (2015). Influence of fine recycled concrete aggregates on the properties of mortars. *Construction and Building Materials*, *81*, 179–186. https://doi.org/10.1016/j.conbuildmat.2015.02.037 ➕ ✏️ 🗑️